A Ligand Protonation Series in Aluminum(III) Complexes of Tridentate Bis(enol)amine Ligand

Nathan A. Phan, James C. Fettinger, and Louise A. Berben*

Department of Chemistry, University of California Davis, Davis, California 95615, United States

Supporting Information

ABSTRACT: A series of aluminum(III) complexes supported by the tridentate bis(enol)amine ligand (ONO, 1,1'-azanediylbis(3,3-dimethylbutan-2-one)) in two protonation states have been synthesized and characterized structurally. Reaction of AlCl₃ with singly deprotonated H₂ONO⁻ afforded pseudooctahedral [(H₂ONO⁻)₂Al][AlCl₄] (1). AlCl₃ was also reacted with doubly deprotonated HONO²⁻ to afford the five-coordinate, pseudotrigonal bipyramidal complex (HONO²⁻)AlCl(THF) (2). The reaction of complex 2 with HCl yielded complex 1, which demonstrates reversible protonation of the ligand backbone. Synthesis of an Al(III) complex of ONO³⁻ was not achieved using a variety of Lewis bases. An attempt to deprotonate complex 2 with 'BuOK

(HONO²⁻)AICI(THF) [(HHONO-)2AI]+

Reversible ligand-based proton transfer

yielded [(HONO²⁻)Al](μ -^tBuO) (3), with no change to the ligand protonation state.

■ INTRODUCTION

The most common coordination mode for the ONO ligand (1,1'-azanediylbis(3,3-dimethylbutan-2-one) is as ONO³⁻, where triple deprotonation has been affected. As examples, complexes of P(III), P(V), As(III), and Sb(III) have been reported with various ancillary ligands to fill out their coordination sphere. Redox chemistry associated with ONO³⁻ is generally oxidative and can involve either the ONO³⁻ fragment or the central ion of a complex, and this of course depends on their relative oxidation potentials. As an example, in the case of P(III) in (ONO³⁻)P^{III}, oxidation to a series of (ONO³⁻)P^VX₂ complexes, where X includes H⁻, NHPh, or NH₂, has been documented.³⁻⁶ Analogous to the P(III/V) examples, single reports of As(III/V) and Sb(III/V) interconversion have been reported where the ligand remains as ONO³⁻ throughout the redox processes.⁷⁻⁹

Complexes of the oxidized ligand, ONO-, have also been reported, and these are generally observed when electron transfer occurs concomitant with ligand coordination to the central ion. Coordination of ONO to Si(II), Ge(II), and Sn(II) has been observed in reactions of Si(IV), Ge(IV), and Sn(IV) precursors, 10 respectively, with the deprotonated ONO³⁻. As an example, synthesis of the Si(II)-containing dimer ([ONO⁻]SiR)₂ was performed starting with Si(IV) reagents, RSiCl₃, where R = H, Ph, Cl, or Br. 11 Synthesis of (ONO⁻)₃Bi was achieved from BiCl₃ and ONO³⁻, although the source of six oxidizing equivalents was not identified in that case.12

The (ONO^{3-}) Pn scaffold, where Pn = pnictogen, has also been isolated as an adduct with various transition metal complexes, where the lone pair on the pnictogen can coordinate to a metal as a neutral donor ligand. A series of complexes of (ONO³⁻)P coordinated to Pt, ¹³ Ag, ¹⁴ Mn, ¹⁵ ⁶ Fe, Cr, W, Ni, and Pd¹⁷ have been characterized.

Similarly, the analogous (ONO³⁻)As and (ONO³⁻)Sb scaffold also form adducts with transition metals.

Efforts to probe a range of protonation states on ONO have not been extensively discussed in the literature, and we therefore cannot determine to what extent this chemistry has been explored. As an example report, reaction of $(\eta^3$ -ONO³⁻)P with HOTf or MeOH affords $[(\eta^2 - ONO^{2-})P]OTf(A)$ or $(\eta^2 - ONO^{2-})P$ ONO²⁻)P(OMe) (B), respectively, and in each molecule, the HONO²⁻ ligand is asymmetric and protonated at one of the carbon atoms adjacent to the N donor. One of the O donors dissociated from the P(III) center, and protonation was not shown to be reversible (Scheme 1).8 Reaction of the P(V) complex $(\eta^3$ -ONO³⁻)PCl₂ with TASF (tris(dimethylamino)sulfonium difluorosiliconate) gave $(\eta^3$ -HONO²⁻)PF₃ (C). Again, the resulting η^3 -HONO²⁻ is asymmetric, protonated at

Scheme 1. Summary of Previous Reports on Protonation Chemistry of ONO³⁻ (In Each Complex the Ligand Is HONO²⁻)

Special Issue: Organometallic Complexes of Electropositive Elements for Selective Synthesis

Received: August 29, 2018 Published: October 15, 2018

one of the C atoms and neither further deprotonation nor reprotonation chemistry was discussed. In that case, three electron-withdrawing fluoro ligands render P(V) more electrophilic than in **A** or **B** and so η^3 -HONO²⁻ is accessed. Partial deprotonation chemistry has also been initiated beginning at the H₃ONO ligand before coordination to a metalloid. In both of those examples, the asymmetric ligand was observed in $[(\eta^2$ -HONO²⁻)E]₂, where E = Ge(IV) or Sn(IV) (**D**), and further deprotonation or reprotonation efforts were not explicitly described.

In this work, we explore the effect on ONO ligand chemistry of employing an electrophilic central ion such as Al(III), which might form stronger ionic interactions with ONO to stabilize the metal-ligand interaction with HONO²⁻ and H₂ONO⁻ ligands and to enable interconversion between protonation states. Recent work on the chemistry of noninnocent ligands has demonstrated that both electron transfer and proton transfer can often be accessed in combination with a suitable central supporting ion. 18 To determine whether additional protonation states of ONO could be accessed in this report, we employed Al(III). The stability of Al(III) to both oxidation and reduction makes it ideal to support a wide range of charge and protonation states as has been demonstrated using ligands such as iminopyridine, ¹⁹ bis(imino)pyridines, ²⁰ α -diimines, ²¹ dpp-BIAN, ²² bis(pyrazolyl)pyridine, ^{18b} and amidobis-(phenolate). ²³ Here, Al(III) enables us to introduce two additional electronic structures for the protonation states of ONO: HONO²⁻ and H₂ONO⁻, along with interconversion of these compounds in acid-base reactions (Scheme 2).

Scheme 2. Potential Protonation States of ONO (Blue Labels Denote Protonation States in This Work; R = ^tBu)

However, the ubiquitous ONO^{3-} protonation state is not accessible. We also explore the ligand-based oxidation and reduction chemistry using cyclic voltammetry and the reaction chemistry of the $HONO^{2-}$ and H_2ONO^- complexes.

RESULTS AND DISCUSSION

Synthesis of Complexes 1–4. Synthesis of Al complexes containing the ONO ligand have been achieved by deprotonating H_3ONO with potassium hydride (KH). Deprotonation of H_3ONO with 1 equiv of KH, followed by the addition of AlCl₃ in THF, resulted in formation of the orange compound, which was identified as a pseudo-octahedral complex, $[(H_2ONO^-)_2Al][AlCl_4]$ (1), in which the two ligands are each deprotonated once (Scheme 3). The site of deprotonation at one of the α -carbons is evident in the 1H NMR spectroscopic measurements, which are consistent with an asymmetric electronic structure for H_2ONO^- (Figure S1). The methylene and vinylic protons flanking the amine appear with three distinct chemical shifts. The vinylic proton is a

Scheme 3. Synthesis of 1-3

doublet at 4.78 ppm ($J_{\rm HH}=5.1$ Hz); one methylene proton appears as a doublet of doublets (3.97 ppm, $J_{\rm HH}=19.1$ and 5.1 Hz), and the other methylene proton appears as a doublet at 3.76 ppm ($J_{\rm HH}=19.1$ Hz). The vinylic proton and the first methylene proton are split by the N–H proton, which appears as a singlet resonance at 5.18 ppm, and the methylene protons split each other. The IR spectrum shows an N–H stretch at 3264 cm⁻¹, a C=O band at 1657 cm⁻¹, and a C–O band at 1095 cm⁻¹ (Figure S2).

Reaction between $\rm H_3ONO$ and 2 equiv of KH over 2 h was followed by addition of AlCl₃ in THF, and this gave a purple-colored solution. Upon workup, a five-coordinate pseudotrigonal bipyramidal complex (HONO²⁻)AlCl(THF) (2) was isolated in 70% yield (Scheme 3). Both α -carbon positions are deprotonated, and the ligand appears symmetric when probed by 1 H NMR spectroscopy (Figure S3). The vinylic C–H resonance is observed at 4.87 ppm as a doublet ($J_{\rm HH}=1.99$ Hz), and the N–H resonance appears as a singlet at 3.28 ppm. The IR spectrum shows an N–H stretch at 3271 cm⁻¹, the sp² C–H absorption band at 3098 cm⁻¹, and a CO band at 1108 cm⁻¹ (Figure S4). To probe the potential for exchange of ligand H atoms, the NMR spectra of complexes 1 and 2 were recorded on solutions exposed to $\rm D_2$ for 24 h. No evidence for exchange was observed.

The ONO³⁻ charge state has been observed in many previous reports, and in an attempt to obtain an Al complex with ONO³⁻, reaction between $\rm H_3ONO$ and 3 equiv of KH over 2 h was followed by addition of AlCl₃ dissolved in THF. A mixture of unidentifiable products was observed using proton NMR spectroscopy. Deprotonation of 2 was also explored in efforts to isolate Al(III) complexes containing fully deprotonated ONO³⁻. Reaction of 2 with KH or Et₃N afforded no change to 2. Reaction of 2 with *n*BuLi yielded a color change from purple to pale yellow, but the resulting ¹H NMR spectrum contained large numbers of resonances in the alkyl region, which suggested multiple products and decomposition. Reaction of 2 with ¹BuOK yielded the dimeric complex $[(HONO^{2-})Al]_2(\mu$ -¹BuO)₂ (3), in which the HONO²⁻ ligand

in 2 has not been deprotonated, but KCl has been eliminated as byproduct to yield an Al_2O_2 diamond core structure (Scheme 3 and Figures S5 and S6).

In a series of reactions, we explored the possibility of accessing a protonation series with either one ligand per Al center, as in 2, or with two ligands per Al center, as in 1. Reaction of 1 with 1 equiv of Et₃N successfully deprotonated H₂ONO⁻ to HONO²⁻, but rearrangement of the metal-ligand connectivity afforded 2 in 52% yield. We reasoned that exchange of the [AlCl₄] counteranion in 1 with anions such as PF₆ or CF₃SO₃ may prevent formation of 2; however, reaction of both NaPF₆ and NaCF₃SO₃ with 1 afforded intractable mixtures. Complex 2 can be selectively protonated at just one of the α -enolate carbon atoms in a reaction with 1 equiv of HCl dissolved in ether. In that reaction, rearrangement of metal-ligand connectivity also occurs so that the bis(ligand) complex 1 was obtained in 42% yield (Scheme 3). The same reactivity was observed with weaker acids such as [HDMAP][BF₄] ($pK_a = 13.6$ in THF, ²⁴ Figure S7). Thus far, we have been unable to generate a protonation series with a single ligand bound to the Al center.

The resistance of 2 toward deprotonation led us to explore the effects of providing additional donating ligands to the Al(III) center to potentially stabilize the ONO³⁻ protonation state. We explored reaction of 2 with bidentate ligands oxalate, bipyridine, and 2,4-di-tert-butylcatecholate but detected no reaction in each case. The reaction of 2 with 2 equiv of monodentate 2,2,6,6-tetramethylpiperidine-N-oxyl (TEMPO) afforded [(HONO²⁻)Al(TEMPO)(TEMPOH)] (4) in 84% yield. The protonation state of the HONO²⁻ ligand is unchanged in the product as compared with the reactant. The ¹H NMR spectrum of 4 supports the ligand assignment as symmetric with a protonated N donor atom (Figure S8): a vinylic C-H resonance is observed at 6.85 ppm as a singlet and the protonated HONO²⁻ N-H resonance at 9.51 ppm in proton NMR spectra. Two TEMPO ligands coordinate the Al center, and one of those appears to be protonated. In the proton NMR spectrum, the TEMPOH N-H resonance appears at 6.53 ppm. Previous reports of TEMPO protonated at the N-H position include complexes of B, 25 Ni, 26 Zr, 27 and Ir, 28 and those TEMPOH N-H resonances were observed at 7.25, 7.62, 7.36, and 12.32 ppm, respectively. Broad IR absorption bands appear at 3403 and 3255 cm⁻¹ and are reasonably attributed to the N-H bonds in HONO²⁻ and in TEMPOH, respectively.

We also attempted to elucidate some details of the mechanism for formation of 4 which contains both an anionic η^1 -TEMPO ligand and a neutral, protonated η^1 -TEMPOH ligand coordinated to the Al center (Scheme 4). Formally, each TEMPO radical has been reduced by one electron in 4, but the

Scheme 4. Synthesis of 4

charge state of the ONO ligand remains unchanged between reactant and product. We propose that reduction of TEMPO may be coupled with the oxidation and dissociation of the chloro ligand which is not present in 4. TEMPO is a strong oxidizing agent ($E^{\circ} = 1.24 \text{ V vs SCE}$), ²⁹ and Cl⁻ is oxidized at 1.12 V vs SCE, ³⁰ so it is possible that the chloro ligand is oxidized to Cl₂, and this would provide one electron toward the observed two-electron reduction. Indeed, reaction solutions are initially green-brown in color and become brown upon exposure to vacuum, which suggests that chlorine gas is formed. The synthesis of 4 was repeated in the presence of the olefins cyclohexene, 9,10-dihydroanthracene, and styrene in an attempt to isolate chlorinated products; however, none was detected by proton NMR spectroscopy or GC-MS. The unreacted olefins were observed in those spectra.

We further reasoned that formation of protonated TEMPOH may occur by abstraction of H• from THF solvent: the reaction yield of 4 is consistently 65-84%, and so it is unlikely that H^o is derived from the ligand. A H^o transfer would also account for the second electron. Protonated TEMPO Al complexes have been previously observed by Hayton and co-workers,³¹ and in those examples, the proton is derived either from the oxidation of alcohols or from 9,10dihydroanthracene. Accordingly, reaction of 2 with 2 equiv of TEMPO was performed in THF-d₈, and the product was investigated using ¹H NMR spectroscopy (Figure S10). No deuterated products were detected. We also prepared 2-d₈ using THF- d_8 as solvent so that the solvate THF molecule is deuterated (Figure S9). The reaction of $2-d_8$ with 2 equiv of TEMPO was performed in benzene-d₆, and the ¹H NMR spectrum revealed the disappearance of the N-H resonance at 6.53 ppm (Figure S10). The reaction suggests that, in the synthesis of 4, TEMPO is protonated via H* abstraction from the solvate THF molecule in an intramolecular process. The reaction of 2 with 2 equiv of TEMPO was also performed in benzene-d₆, and the ¹H NMR spectrum revealed no deuterium incorporation (Figure S10).

Solid-State Structures. Single crystals of 1 were grown as pale orange plates from a concentrated toluene solution held at $-15\,^{\circ}\text{C}$ overnight (Figure 1, Table 1, and Table S1). The solid-state structure of 1 was characterized by single-crystal X-ray diffraction. The bond lengths and angles in 1 suggest that the H_2ONO^- ligand is deprotonated once at an α -carbon position and is monoanionic. The anionic ligand charge

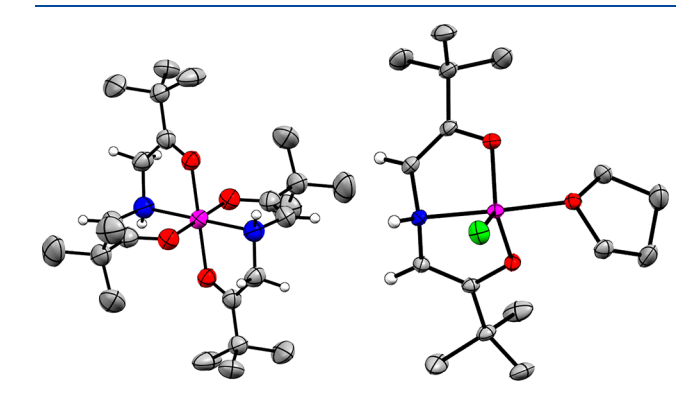


Figure 1. Solid-state structures of (left) $[(H_2ONO^-)_2Al]^+$ in **1** and (right) (HONO²⁻)AlCl(THF) in **2**. Pink, red, blue, gray, green, and white represent Al, O, N, C, Cl, and H atoms, respectively. Thermal ellipsoids at 50% probability. t-Bu H atoms omitted.

Table 1. Selected Average Bond Distances for 1, 2, and 3

	1	2	3	$(ONO^{3-})P(H)_2^4$
М-О	1.836(3)	1.773(10)	1.7749(9)	1.721(1)
	1.978(3)	1.7745(10)		1.699(2)
M-N	2.006(4)	2.0592(10)	2.1210(15)	1.676(2)
C-O	1.315(5)	1.3624(15)	1.3468(15)	1.384(2)
	1.209(5)	1.3450(15)		
C-N	1.456(5)	1.4665(15)	1.4591(18)	1.400(2)
	1.494(5)	1.4641(15)		
C-C	1.347(6)	1.3456(18)	1.332(2)	1.325(2)
	1.513(6)	1.3438(17)		

appears localized on one enolate O donor, where the Al–O bond length is 1.836(3) Å and the C–O bond length is 1.315(5) Å. The other Al–O and C–O bonds in 1 are 1.978(3) and 1.209(5) Å, respectively.

Single crystals of **2** suitable for X-ray diffraction were grown as pale purple plates from a concentrated solution of 1:1 hexanes/toluene held at $-15\,^{\circ}$ C overnight (Figure 1, Table 1, and Table S1). Based on the Al ligand bond angles, we calculated the τ_5 value for **1** as 0.70, and this indicates that the Al center is best described as pseudotrigonal pyramidal in geometry.³² The bond lengths for **2** suggest that the ligand framework is symmetric, and that both α -carbon positions are deprotonated. The ligand is dianionic, as evidenced by the elongated C–O bonds, 1.3624(15) and 1.3540(15) Å, and the shortened Al–O bonds, 1.7723(10) and 1.745(1) Å. Despite the higher overall anionic ligand charge in **2**, relative to **1**, the Al–N bond length is approximately the same, at 2.0592(10) compared with 2.006(4) Å.

Single crystals of 3 were grown as blue blocks from a concentrated toluene solution held at -15 °C overnight (Figure 2, Table 1, and Table S1). The Al-O and C-O bond

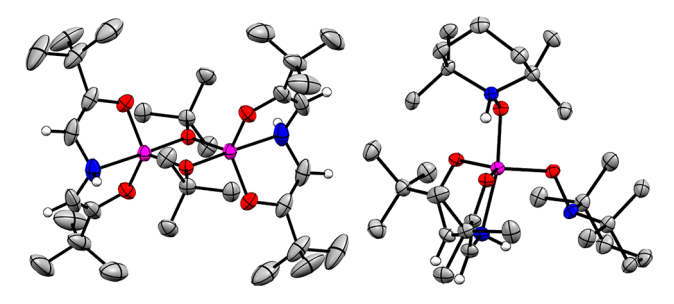


Figure 2. Solid-state structures of (left) $[(HONO^2-)Al]_2(\mu^-tBuO)_2$ in 3 and (right) $(HONO^2-)Al(TEMPO)(TEMPOH)$ in 4. Pink, red, blue, gray, and white represent Al, O, N, C, and H atoms, respectively. Thermal ellipsoids at 50% probability. *t*-Bu H atoms and TEMPO C—H atoms omitted.

lengths in 3 are very similar to those in 2, at 1.7749(9) and 1.3468(15) Å, respectively, and these comparisons suggest that the best assignment for 3 is with HONO²⁻, in agreement with spectroscopic data. Single crystals of 4 were grown as blue needles from a concentrated solution of 1:1 hexanes/toluene held at 15 °C overnight. The τ_5 value of 4 is 0.72, consistent with a pseudotrigonal pyramidal geometry.³² The average Al–O and C–O bond lengths in 4 are similar to those in 2, at 1.8200(11) and 1.3486(19) Å, respectively. These metrics, along with the proton NMR and IR data (Figure S8), confirm that the ligand is best described as HONO²⁻.

Electrochemical Studies. Electrochemical measurements were performed using cyclic voltammetry (CV) of complexes 1 and 2 in solutions of 0.3 M Bu₄NPF₆ THF solution (Figure 3).

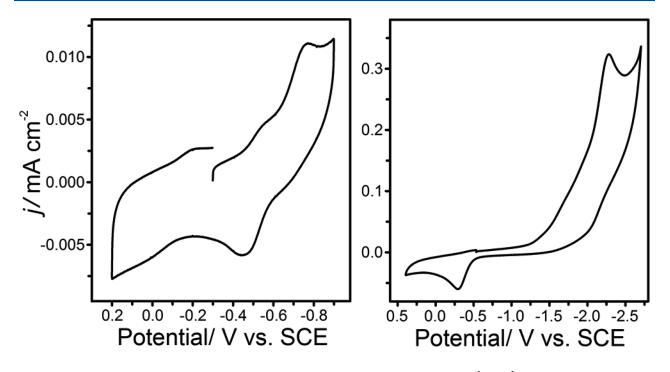


Figure 3. Cyclic voltammograms of 0.5 mM 1 (left) and 1 mM 2 (right) in 0.3 M Bu_4NPF_6 THF. Scan rate = 100 mV s⁻¹, glassy carbon working electrode.

The CV of 1 has two quasi-reversible couples that we assigned as ligand-based reduction events. The first couple occurs at -0.14 V vs SCE, and we assign this as $\text{H}_2\text{ONO}^{0/-}$ (Scheme 5).

Scheme 5. Potentially Accessible Charge States of the H₂ONO (Left) and HONO (Right) Ligands

The second couple was observed at -0.51 V, and we assigned that as $H_2ONO^{-/2-}$. One further irreversible reduction event was observed with $E_p = -0.76$ V. No further processes were observed when the CV was scanned in the anodic direction. As might be expected, reduction of 2 which has only one proton, occurs at more negative potential than the reduction of 1. The CV of **2** shows one irreversible reduction event with $E_p = -2.26$ V, and we assign this to the HONO^{2-/3-} couple in **2**. Loss of Cl⁻ from the Al center or loss of H[•] from the ligand upon reduction could account for the irreversibility of the event at -2.26 V. There is an irreversible oxidation event at $E_{\rm p}$ = -0.32 V which we attribute to oxidation of HONO²⁻ into HONO⁻. This event persists when the CV is scanned in the anodic direction first. Chemical oxidation of 2 was attempted using ferrocenium hexafluorophosphate, and that reaction resulted in the loss HONO²⁻ ligand from Al(III), which is consistent with the irreversible electrochemical behavior.

CONCLUSIONS

The combination of the ONO ligand platform with highly electrophilic Al(III) has allowed the isolation of ONO ligand protonation states $\rm HONO^{2-}$ and $\rm H_2ONO^{-}$, along with their interconversion using Brønsted bases and acids. The substitution of ancillary chloro ligands in the $\rm HONO^{2-}$ complex 2 with oxo donors such as TEMPO and μ^2 - $^t\rm BuO$ is

reported. Structural characterization of each of the reported compounds shows that the $\rm H_2ONO^-$ is deprotonated at one of the α C atoms to provide an asymmetric ligand form with unequal C–O and C–C bond lengths. The ligand form $\rm HONO^{2-}$ is symmetric and deprotonated twice at equivalent C atoms. Previous explorations of the chemistry of the ONO ligand have revealed numerous reports of the ONO³⁻ and the oxidized ONO⁻ forms, and the present work has expanded on the available ligand protonation chemistry to demonstrate the influence of electrophilic Al(III) on ligand-based proton and electron transfer chemistry.

EXPERIMENTAL SECTION

Preparation of Compounds. All manipulations were carried out under a dinitrogen atmosphere using a standard Schlenk line and glovebox techniques. All chemicals were purchased from VWR International, Acros, Alpha Aesar, or Cambridge Isotopes. Bulk solvents were deoxygenated and dried by sparging with argon gas followed by passage through an activated alumina column. Deuterated solvents and other liquid reagents were degassed with dinitrogen and stored over activated 3 Å sieves prior to use. H₃ONO was synthesized in accordance with a reported procedure. ⁵

 $[(H_2ONO^-)_2AI][AICI_4]$ (1). A solution of H_3ONO (259 mg, 1.22 mmol) in THF (2 mL) was held at -78 °C while KH (58.1 mg, 1.45 mmol) was added. The solution was stirred for 1 h as it warmed to room temperature and then cooled again to -78 °C along with a solution of AlCl₃ (188 mg, 1.42 mmol) in THF (2 mL). The solution of "H2ONO" was added to the stirring solution of AlCl3 dropwise and warmed to room temperature with stirring over 2 h. The resulting orange solution was evaporated to dryness, rinsed in 2 mL hexanes, extracted into 5 mL benzene, and filtered through Celite. The filtrate was evaporated to dryness to afford 1 as a light orange powder (263 mg, 70%). Crystals suitable for X-ray diffraction were grown from a concentrated toluene solution at -15 °C overnight. ¹H NMR (400 MHz, C_6D_6) δ 5.18 (s, 2H, CH), 4.78 (d, J = 5.1 Hz, 2H, NH), 3.97 (dd, J = 19.1, 5.1 Hz, 2H, CH_2), 3.76 (d, J = 19.0 Hz, 2H, CH_2), 1.16 (s, 20H, C(CH₃)₃), 0.74 (s, 19H, C(CH₃)₃). ¹³C NMR (600 MHz, C_6D_6) δ 170.37, 100.25, 58.09, 43.39, 34.79, 27.92, 27.84, 25.28. IR (KBr; cm⁻¹): 3305 (w, NH), 3264 (m, NH), 3090 (w, CH), 2970 (s, CH), 2911 (m), 2873 (m), 1715 (m), 1657 (s, C = O), 1623 (m), 1480 (m), 1462 (m), 1414 (w), 1390 (m), 1370 (s), 1344 (m), 1297 (m), 1221 (m), 1161 (m), 1107 (m), 1095 (s, C-O). UV-vis spectrum (THF) $\lambda_{\rm max}$ ($\varepsilon_{\rm M}$): 328 (2513), 447 (5770) nm (L mol⁻¹cm⁻¹). Anal. Calcd C₂₄H₄₄Al₂Cl₄N₂O₄: C, 46.49; H, 7.14; N, 4.52. Found: C, 43.55; H, 6.79; N, 4.04.

(HONO²⁻)AlCl(THF) (2). A solution of H₃ONO (295 mg, 1.39 mmol) in THF (2 mL) was held at -78 °C, while KH was added (128 mg, 3.19 mmol). The solution was stirred for 1 h as it warmed to room temperature and then cooled again to $-78~^{\circ}\text{C}$ along with a solution of AlCl₃ (185 mg, 1.39 mmol) in THF (2 mL). The solution of "HONO" was added to the stirring solution of AlCl₃ dropwise and warmed to room temperature with stirring over 2 h. The resulting purple solution was evaporated to dryness, extracted into hexane (5 mL), and filtered through Celite to remove salts. The filtrate was evaporated to dryness, and 2 was isolated as a light purple powder (357 mg, 75%). Crystals suitable for X-ray diffraction were grown by cooling a concentrated 1:1 hexane/toluene solution at -15 °C overnight. ¹H NMR (400 MHz, C_6D_6): δ 4.87 (d, J = 1.99 Hz, 2H, CH), 4.04 (s, 4H, THF), 3.28 (s, 1H, NH), 1.17 (s, 22H, THF and $C(CH_3)_3$). ¹³C NMR (600 MHz, C_6D_6): δ 168.14, 101.87, 71.51, 34.88, 27.97, 25.07. IR (KBr, cm⁻¹): 3271 (m, NH), 3098 (w, CH), 2963 (s), 2906 (m), 2869 (m), 1666 (w), 1642 (s), 1481 (m), 1458 (w), 1389 (m), 1356 (m), 1331 (s), 1219 (m), 1161 (m), 1131 (m), 1108 (m, C-O) 1092 (s), 1020 (s). UV-vis spectrum (THF) λ_{max} $(\varepsilon_{\rm M})$: 308 (1251), 454 (105), 562 (28) nm ($\bar{\rm L}$ mol $^{-1}$ cm $^{-1}$). Anal. Calcd for C₁₆H₂₉AlClNO₃: C, 55.58; H, 8.45; N, 4.05. Found: C, 55.39; H, 8.08; N, 4.32.

[(HONO²-)Al]₂(μ-¹BuO)₂ (3). A solution of complex 2 (106 mg, 0.307 mmol) in THF (2 mL) was prepared. A second solution of ¹BuOK (37.4 mg, 0.333 mmol) in THF (1 mL) was then added to the first solution. The resulting blue solution was evaporated to dryness and extracted into benzene (5 mL) and filtered through Celite to remove salts. The filtrate was evaporated to dryness, and 3 was isolated as a light blue powder (93.3 mg, 49%). ¹H NMR (400 MHz, C_6D_6): δ 4.96 (d, J = 2.17 Hz, 4H, CH), 3.60 (s, 2H, N–H), 1.49 (s, 18H, C(CH₃)₃), 1.21 (m, 36H, C(CH₃)₃). ¹³C NMR (600 MHz, C_6D_6): δ 168.65, 99.93, 73.01, 34.62, 31.28, 27.79. IR (KBr, cm⁻¹): 3295 (w NH), 3093 (w, CH), 2963 (s), 2924 (m), 2905 (m), 2869 (m), 1642 (s), 1542 (w), 1481 (m), 1460 (m), 1421 (w), 1387 (m), 1370 (m), 1343 (s), 1240 (m), 1220 (s), 1183 (m), 1164 (m), 1142 (m), 1112 (m, C–O), 1030 (m), 1004 (s). UV–vis spectrum (THF) λ_{max} (ε_{M}): 323 (29), 457 (17) nm (L mol⁻¹ cm⁻¹). Anal. Calcd for $C_{32}H_{60}Al_2N_2O_6\cdot H_2O: C$, 59.98; H, 9.75; N, 4.37. Found: C, 59.65; H, 8.53 N, 4.47.

(HONO²⁻)AI(TEMPO)(TEMPOH) (4). A solution of complex 2 (44.5 mg, 0.129 mmol) in THF (1 mL) was prepared. A second solution of TEMPO (44.9 mg, 0.287 mmol) in THF (1 mL) was then added to the first solution. The resulting brown solution was evaporated to dryness and extracted into benzene (5 mL) and filtered through Celite. The filtrate was evaporated to dryness, and 4 was isolated as a light brown powder (60.2 mg, 74%). ¹H NMR (400 MHz, C_6D_6): δ 9.51 (s, 1H), 6.85 (s, 2H), 6.53 (s, 1H), 1.82 (s, 6H), 1.56 (d, J = 8.0 Hz, 6H), 1.38 (s, 14H), 1.17–1.12 (m, 30H). ¹³C NMR (600 MHz, C_6D_6): δ 200.13, 116.28, 68.17, 60.05, 39.20, 38.25, 30.35, 27.14, 20.37, 19.95, 15.90. IR (KBr, cm⁻¹): 3403 (w, NH), 3255 (w, NH), 2961 (m, CH), 2927 (m), 2871 (m), 1567 (m), 1535 (m), 1460 (m), 1438 (m), 1421 (m), 1386 (m), 1375 (m), 1366 (m), 1298 (s), 1226 (m), 1103 (s, C-O), 1064 (m), 1014 (m). UV-vis spectrum (THF) λ_{max} (ε_{M}): 323 (1013), 434 (6829), 452 (6960) nm (L mol⁻¹ cm⁻¹). Anal. Calcd for C₃₀H₅₈AlN₃O₄·2H₂O: C, 61.30; H, 10.63; N, 7.15. Found: C, 60.28; H, 10.04; N, 7.04.

Physical Measurements. Elemental analyses were performed by the Microanalytical Laboratory at The University of California, Berkeley. ¹H and ¹³C NMR spectra were recorded at ambient temperature using a Varian 600 MHz or Bruker 400 MHz spectrometer. Chemical shifts were referenced to residual solvent. Infrared spectra were recorded on a Bruker Alpha Infrared spectrometer (2 cm⁻¹ resolution). GC-MS measurements were conducted on an Agilent 6890N GC with a 5973N MS. UV-vis spectra were recorded in THF solution using an Agilent 8453 UV-vis spectrophotometer (Figure S11).

Cyclic voltammograms were recorded in a nitrogen-filled glovebox. A CH Instruments model 620D electrochemical analyzer with a glassy carbon working electrode (CH Instruments, nominal surface area of 0.071 cm²), a platinum wire auxiliary electrode, and a Ag/AgNO $_3$ (0.001 M) nonaqueous reference electrode with a Vycor tip was used. All potentials are referenced to the SCE couple, and ferrocene was used as an internal standard, where the $E_{1/2}$ value of ferrocene/ferrocenium is +0.56 V vs SCE in 0.3 M $\rm Bu_4NPF_6$ THF solution. 33 $\rm Bu_4NPF_6$ was recrystallized from ethanol and placed under vacuum for 72 h before electrolyte solutions were made. Electrolyte solutions were stored over 3 Å molecular sieves for at least 48 h before use. Sieves were activated by heating under vacuum at 270 °C for at least 72 h. All other reagents were purchased from commercial vendors and used as received.

X-ray diffraction studies were carried out on a Bruker SMART APEX Duo and Kappa Duo diffractometer equipped with a CCD detector. The Measurements were carried out at $-175\,^{\circ}\mathrm{C}$ using Mo Ka (0.71073 Å) radiation and Cu Ka (1.54178 Å) radiation. Crystals were mounted on a glass capillary or Kaptan Loop with Paratone-N oil. Initial lattice parameters were obtained from a least-squares analysis of more than 100 centered reflections; these parameters were later refined against all data. Data were integrated and corrected for Lorentz polarization effects using SAINT and were corrected for absorption effects using SADABS2.3. Space group assignments were based upon systematic absences, E statistics, and successful refinement of the structures. Structures were solved by direct methods with

the aid of successive difference Fourier maps and were refined against all data using the SHELXTL 2014/7 software package. Thermal parameters for all non-hydrogen atoms were refined anisotropically. Hydrogen atoms, where added, were assigned to ideal positions and refined using a riding model with an isotropic thermal parameter 1.2 times that of the attached carbon atom (1.5 times for methyl hydrogens).

ASSOCIATED CONTENT

S Supporting Information

The Supporting Information is available free of charge on the ACS Publications website at DOI: 10.1021/acs.organomet.8b00628.

Tables of crystallographic data and interatomic distances and angles; Figures S1–S11 (PDF)

Accession Codes

CCDC 1846128–1846131 contain the supplementary crystallographic data for this paper. These data can be obtained free of charge via www.ccdc.cam.ac.uk/data_request/cif, or by emailing data_request@ccdc.cam.ac.uk, or by contacting The Cambridge Crystallographic Data Centre, 12 Union Road, Cambridge CB2 1EZ, UK; fax: +44 1223 336033.

AUTHOR INFORMATION

Corresponding Author

*E-mail: laberben@ucdavis.edu.

ORCID 6

James C. Fettinger: 0000-0002-6428-4909 Louise A. Berben: 0000-0001-6461-1829

Notes

The authors declare no competing financial interest.

ACKNOWLEDGMENTS

We thank the National Science Foundation for support of this work with award CHE-1763821. Preliminary results were obtained with support of a New Directions Grant from the University of California Davis Academic Senate. The National Science Foundation provided the dual source X-ray diffractometer (CHE-1531193) and the NMR instrumentation (DBIO-722538).

REFERENCES

- (1) Culley, S. A.; Arduengo, A. J. Synthesis and Structure of the First 10-P-3 Species. J. Am. Chem. Soc. 1984, 106, 1164–1165.
- (2) Culley, S. A.; Arduengo, A. J. The Synthesis and Structure of the First 10-As-3 species. *J. Am. Chem. Soc.* 1985, 107, 1089–1090.
- (3) Arduengo, A. J.; Breker, J.; Davidson, F.; Kline, M. Dihalo Derivatives of 5-coordinate Hypervalent Phosphorus Compounds. *Heteroat. Chem.* **1993**, *4*, 213–221.
- (4) Dunn, N. L.; Ha, M.; Radosevich, A. T. Main Group Redox Catalysis: Reversible $P^{\rm III}/P^{\rm V}$ Redox Cycling at a Phosphorus Platform. *J. Am. Chem. Soc.* **2012**, *134*, 11330–11333.
- (5) McCarthy, S. M.; Lin, Y.-C.; Devarajan, D.; Chang, J. W.; Yennawar, H. P.; Rioux, R. M.; Ess, D. H.; Radosevich, A. T. Intermolecular N-H Oxidative Addition of Ammonia, Alkylamines, and Arylamines to a Planar σ^3 -Phosphorus Compound via an Entropy-Controlled Electrophilic Mechanism. *J. Am. Chem. Soc.* **2014**, *136*, 4640–4650.
- (6) Lin, Y.-C.; Gilhula, J. C.; Radosevich, A. T. Nontrigonal Constraint Enhances 1,2-addition Reactivity of Phosphazenes. *Chem. Sci.* **2018**, *9*, 4338–4347.
- (7) Stewart, C. A.; Harlow, R. L.; Arduengo, A. J. Chemistry and Structure of the First 10-Sb-3 Species. J. Am. Chem. Soc. 1985, 107, 5543–5545.

(8) Arduengo, A. J.; Stewart, C. A.; Davidson, F.; Dixon, D. A.; Becker, J. Y.; Culley, S. A.; Mizen, M. B. The Synthesis, Structure, and Chemistry of 10-Pn-3 Systems: Tricoordinate Hypervalent Pnictogen Compounds. *J. Am. Chem. Soc.* **1987**, *109*, 627–647.

- (9) Driess, M.; Dona, N.; Merz, K. Novel Hypervalent Complexes of Main-group Metals by Intramolecular Ligand→Metal Electron Transfer. Chem. Eur. J. 2004, 10, 5971–5976.
- (10) Bettermann, G.; Arduengo, A. J. The Chemistry and Structure of a 10-Sn-4 System: Pseudo-trigonal-bipyramidal 4-coordinate, 10-electron Tin Centers. *J. Am. Chem. Soc.* **1988**, *110*, 877–879.
- (11) Driess, M.; Muresan, N.; Merz, K. A Novel Type of Pentacoordinate Silicon Complexes and Unusual Ligand coupling by Intramolecular Electron Transfer. *Angew. Chem., Int. Ed.* **2005**, *44*, 6738–6741.
- (12) Stewart, C. A.; Calabrese, J. C.; Arduengo, A. J. Synthesis and Structure of the First 20-Bi-9 System: A Discrete Nine-coordinate 20-electron Bismuth. *J. Am. Chem. Soc.* **1985**, *107*, 3397–3398.
- (13) Arduengo, A. J., III; Stewart, C. A.; Davidson, F. Reversible transformation of 10-P-3 ADPO to an 8-P-3 ADPO PtI₂ Adduct. *J. Am. Chem. Soc.* **1986**, *108*, 322–323.
- (14) Arduengo, A. J.; Dias, H. V. R.; Calabrese, J. C. A Novel Mode of Coordination for Phosphorus. *J. Am. Chem. Soc.* **1991**, *113*, 7071–7072.
- (15) Arduengo, A. J.; Lattman, M.; Calabrese, J. C.; Fagan, P. J. Complexes of Tricoordinate Hypervalent Pnictogens with (pentamethylcyclopentadienyl)ruthenium. *Heteroat. Chem.* **1990**, *1*, 407–417.
- (16) Arduengo, A. J.; Lattman, M.; Dias, H. V. R.; Calabrese, J. C.; Kline, M. Pentacoordinate 10-electron Pnictogen-manganese Adducts: Verification of the 10-Pn-3 Arrangement in ADPnO Molecules. *J. Am. Chem. Soc.* **1991**, *113*, 1799–1805.
- (17) Arduengo, A. J.; Rasika Dias, H. V.; Calabrese, J. C. Coordination Chemistry of ADPO. *Phosphorus, Sulfur Silicon Relat. Elem.* **1994**, 87, 1–10.
- (18) (a) Thompson, E. J.; Berben, L. A. Electrocatalytic Hydrogen Production by an Aluminum(III) Complex: Ligand-Based Proton and Electron Transfer. Angew. Chem., Int. Ed. 2015, 54, 11642-11646. (b) Sherbow, T. J.; Fettinger, J. C.; Berben, L. A. Control of Ligand pK_a Values Tunes the Electrocatalytic Dihydrogen Evolution Mechanism in a Redox-Active Aluminum(III) Complex. Inorg. Chem. 2017, 56, 8651-8660. (c) Haddad, A. Z.; Garabato, B. D.; Kozlowski, P. M.; Buchanan, R. M.; Grapperhaus, C. A. Beyond Metal-Hydrides: Non-Transition-Metal and Metal-Free Ligand-Centered Electrocatalytic Hydrogen Evolution and Hydrogen Oxidation. J. Am. Chem. Soc. 2016, 138, 7844-7847. (d) Solis, B. H.; Maher, A. G.; Dogutan, D. K.; Nocera, D. G.; Hammes-Schiffer, S. Nickel Phlorin Intermediate Formed by Proton- Coupled Electron Transfer in Hydrogen Evolution Mechanism. Proc. Natl. Acad. Sci. U. S. A. 2016, 113, 485-492. (e) Henthorn, J. T.; Lin, S.; Agapie, T. Combination of Redox-Active Ligand and Lewis Acid for Dioxygen Reduction with π -Bound Molybdenum-Quinonoid Complexes. *J.* Am. Chem. Soc. 2015, 137, 1458-1464.
- (19) (a) Myers, T. W.; Kazem, N.; Stoll, S.; Britt, R. D.; Shanmugam, M.; Berben, L. A. A Redox Series of Aluminum Complexes: Characterization of Four Oxidation States Including a Ligand Biradical State Stabilized via Exchange Coupling. *J. Am. Chem. Soc.* 2011, 133, 8662–8672. (b) Myers, T. W.; Berben, L. A. Countercations Direct One- or Two-Electron Oxidation of an Al(III) Complex and Al(III)—Oxo Intermediates Activate C—H Bonds. *J. Am. Chem. Soc.* 2011, 133, 11865–11867.
- (20) (a) Myers, T. W.; Berben, L. A. Aluminum—Amido-Mediated Heterolytic Addition of Water Affords an Alumoxane. *Organometallics* **2013**, *32*, 6647–6649. (b) Myers, T. W.; Berben, L. A. Aluminum—Ligand Cooperative N—H Bond Activation and an Example of Dehydrogenative Coupling. *J. Am. Chem. Soc.* **2013**, *135*, 9988–9990. (c) Myers, T. W.; Berben, L. A. Aluminium-ligand Cooperation Promotes Selective Dehydrogenation of Formic Acid to H₂ and CO₂. *Chem. Sci.* **2014**, *5*, 2771–2777.

(21) (a) Cole, B. E.; Wolbach, J. P.; Dougherty, W. G.; Piro, N. A.; Kassel, W. S.; Graves, C. R. Synthesis and Characterization of Aluminum-α-diimine Complexes over Multiple Redox States. *Inorg. Chem.* **2014**, *53*, 3899–3906. (b) Wilson, H. H.; Koellner, C. A.; Hannan, Z. M.; Endy, C. B.; Bezpalko, M. W.; Piro, N. A.; Kassel, W. S.; Sonntag, M. D.; Graves, C. R. Synthesis and Characterization of Neutral Ligand α-Diimine Complexes of Aluminum with Tunable Redox Energetics. *Inorg. Chem.* **2018**, *57*, 9622–9633.

- (22) (a) Fedushkin, I. L.; Khvoinova, N. M.; Skatova, A. A.; Fukin, G. K. Oxidative Addition of Phenylacetylene through C-H Bond Cleavage To Form the Mg^{II}—dpp-Bian Complex: Molecular Structure of [Mg{dpp-Bian(H)}(C-CPh) (thf)₂] and Its Diphenylketone Insertion Product [Mg(dpp-Bian).—{OC(Ph₂)C-CPh}(thf)]. *Angew. Chem., Int. Ed.* **2003**, 42, 5223—5226. (b) Moskalev, M. V.; Lukoyanov, A. N.; Baranov, E. V.; Fedushkin, I. L. Unexpected Reactivity of an Alkylaluminum Complex of a Non-innocent 1,2-bis[(2,6-diisopropylphenyl)imino]acenaphthene Ligand (dpp-Bian). *Dalton Trans.* **2016**, 45, 15872—15878.
- (23) Szigethy, G.; Heyduk, A. F. Aluminum complexes of the redoxactive [ONO] pincer ligand. *Dalton Trans.* **2012**, *41*, 8144–8152.
- (24) Garrido, G.; Koort, E.; Rafols, C.; Bosch, E.; Rodima, T.; Leito, I.; Roses, M. J. *J. Org. Chem.* **2006**, *71*, 9062–9067.
- (25) Chen, G.-Q.; Daniliuc, C. G.; Kehr, G.; Erker, G. Making Use of the Functional Group Combination of a Phosphane/Borane Lewis Pair Connected by an Unsaturated Four-Carbon Bridge. *Eur. J. Inorg. Chem.* **2017**, 2017, 4519–4524.
- (26) Isrow, D.; Captain, B. Synthesis and Reactivity of a Transition Metal Complex Containing Exclusively TEMPO Ligands: Ni(η 2-TEMPO)2. *Inorg. Chem.* **2011**, *50*, 5864–5866.
- (27) Liu, Y.-L.; Kehr, G.; Daniliuc, C. G.; Erker, G. Utilizing the TEMPO Radical in Zirconocene Cation and Hydrido Zirconocene Chemistry. *Organometallics* **2017**, *36*, 3407–3414.
- (28) Hetterscheid, D. G. H.; Kaiser, J.; Reijerse, E.; Peters, T. P. J.; Thewissen, S.; Blok, A. N. J.; Smits, J. M. M.; de Gelder, R.; de Bruin, B. IrII(ethene): Metal or Carbon Radical? *J. Am. Chem. Soc.* **2005**, 127, 1895–1905.
- (29) Hodgson, J. L.; Namazian, M.; Bottle, S. E.; Coote, M. L. One-Electron Oxidation and Reduction Potentials of Nitroxide Antioxidants: A Theoretical Study. *J. Phys. Chem. A* **2007**, *111*, 13595–13605.
- (30) Atkins, P. *Physical Chemistry*, 6th ed.; W.H. Freeman & Co.: New York, 1997.
- (31) Scepaniak, J. J.; Wright, A. M.; Lewis, R. A.; Wu, G.; Hayton, T. W. Tuning the Reactivity of TEMPO by Coordination to a Lewis Acid: Isolation and Reactivity of $MCl_3(\eta^1\text{-TEMPO})$ (M = Fe, Al). *J. Am. Chem. Soc.* **2012**, *134*, 19350–19353.
- (32) Addison, A. W.; Rao, T. N.; Reedijk, J.; Van Rijn, J.; Verschoor, G. C.Synthesis, structureand spectroscopic properties of copper(II) compounds containing nitrogen—sulphur donor ligands, 1984 Synthesis, structure, and spectroscopic properties of copper(II) compounds containing nitrogen—sulphur donor ligands; the crystal and molecular structure of aqua[1,7-bis(N-methylbenzimidazol-2'-yl)-2,6-dithiaheptane]copper(II) perchlorate. *J. Chem. Soc., Dalton Trans.* 1984, 1349—1356.
- (33) Connelly, N. G.; Geiger, W. E. Chemical Redox Agents for Organometallic Chemistry. Chem. Rev. 1996, 96, 877–910.
- (34) (a) SMART Software Users Guide, version 5.1; Bruker Analytical X-ray Systems, Inc.: Madison, WI, 1999. (b) SAINT Software Users Guide, version 7.0; Bruker Analytical X-ray Systems, Inc.: Madison, WI, 1999. (c) Sheldrick, G. M. SADABS, version 2.03, Bruker Analytical X-ray Systems, Inc.: Madison, WI, 2000. (d) Sheldrick, G. M. SHELXTL, version 6.12; Bruker Analytical X-ray Systems, Inc.: Madison, WI, 1999. (e) International Tables for X-ray Crystallography; Kluwer Academic Publishers: Dordrecht, The Netherlands, 1992; Vol. C.